

Frequency-stabilized semimonolithic frequency doubler with high output power

Yu Luo (罗 玉), Ying Li (李 莹), Changde Xie (谢常德),
Kunchi Peng (彭楚琳), and Qing Pan (潘 庆)

State Key Laboratory of Quantum Optics and Quantum Optics Devices,
Institute of Opto-Electronics of Shanxi University, Taiyuan 030006

Received January 10, 2005

We present a semimonolithic frequency-doubler from 1080 to 540 nm with 80% doubling efficiency and up to 849-mW output power of green light. A frequency-stabilized laser diode (LD) pumped continuous wave (CW) Nd:YAP laser is used as the pump source of the doubler consisting of an α -cut KTP crystal and an input mirror. The frequency stabilities of the output second harmonic wave are better than ± 246 kHz and ± 2.3 MHz in 1 and 30 minutes, respectively, and the intensity fluctuation is less than $\pm 0.65\%$.
OCIS codes: 120.2230, 120.4640, 140.3560.

The frequency-doubled Nd:YAP laser with high output power is an important pumping source for quantum information, quantum optics, and nonlinear optics experiments^[1-6]. Intracavity frequency-doubled^[7-11] and external frequency-doubled lasers^[12-18] are two usual methods to generate continuous second harmonic wave. For the former, the frequency-doubling nonlinear crystal and the active medium of the laser are put in the same resonant cavity, thus the process of frequency doubling possibly affects the stability of the fundamental laser, and eventually the stability of the second harmonic output is correspondingly reduced also. For the latter, the frequency-doubling cavity and the fundamental laser resonant cavity are separated, therefore the influence of each other can be decreased to minimum and both of the cavities can be adjusted to operate in the optimum states. Because 540-nm laser can realize type-II 90° non-critical phase matching in an α -cut KTP crystal, it has become an important pump source of nondegenerate optical parameter amplifiers (NOPAs) producing the two-mode squeezed and entangled states of light^[4-6]. The continuous wave (CW) frequency-doubling from 1080 to 540 nm was firstly demonstrated by Ou *et al.* with a ring doubler outside the laser resonant cavity of fundamental wave, and 85% conversion efficiency with up to 560-mW harmonic power was obtained^[12]. Recently, Hayasaka *et al.* got 22.8-mW, 540-nm green light from 50-mW, 1080-nm diode laser via the similar method^[13]. However, for getting low passive loss, the extremely high quality of the four mirrors constituting the ring frequency-doubling cavity has to be reached, and the alignment of the folded ring cavity is relatively difficult^[12,13]. In this paper, we present a relatively robust design of frequency doubler, which is a standing wave cavity consisting of a semimonolithic KTP crystal and a concave mirror. We paid special attention on the stabilities of the output harmonic wave from the doubler. The solid mechanical configuration and excellent frequency-locking system of Nd:YAP laser provide a high stable fundamental input which is the base ensuring the stability of harmonic output. The output power of 849 mW at 540 nm is obtained under the input power of 1.18 W at 1080 nm, and

the intensity fluctuation is about $\pm 0.65\%$. The directly measured frequency-doubling efficiency is 72%, when the 90% transmission coefficient of output mirror is taken into account it is 80%. The frequency stabilities are better than ± 246 kHz and ± 2.3 MHz in 1 and 30 minutes, respectively.

In order to enhance the conversion efficiency, the passive losses of the cavity must be as low as possible. Considering a variety of requirements, such as low intracavity losses, robust, easier to be aligned and lower cost, we design a semimonolithic doubling cavity with near concentric configuration as shown in Fig. 1. In the figure, M_1 is the input mirror and M_2 is one of the facets of the doubling crystal coated to act as output mirror. r_1 , r_2 and t_1 , t_2 are the power reflection and transmission coefficients of the cavity mirrors M_1 and M_2 for the fundamental wave, respectively. t stands for power transmission coefficient of the fundamental wave in a single pass inside the cavity. P_i and P_r are the input and reflected power of the fundamental wave on and from mirror M_1 , respectively. P_c is the fundamental power inside the cavity. Following Refs. [17,18], we define a cavity reflectance parameter r_m , $r_m = t^2 r_2$, which stands for the fraction of resonating fundamental light left after one round trip inside the cavity. For a low loss cavity, the active loss caused by frequency-doubling process must be taken into account^[18]. If this active loss is small in comparison with P_c , it can be expressed by an additional crystal transmission term t_{SH} ^[18]:

$$t_{SH} = 1 - \eta_{SH}, \quad (1)$$

$\eta_{SH} = \gamma_{SH} P_c$ is the conversion efficiency from the resonant fundamental wave to the second harmonic wave.

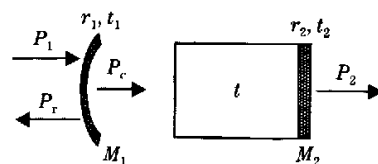


Fig. 1. Frequency-doubling cavity. M_1 : fundamental input mirror; M_2 : harmonic output mirror.

γ_{SH} is the nonlinear conversion factor^[19]:

$$\gamma_{SH} = Klk_1 \exp[-a'l]h(\sigma, \beta, \kappa, \xi, \mu), \quad (2)$$

and

$$K = (128\pi^2\omega_1^2 d_{eff}^2)/(c^3 n_1^2 n_2), \quad \alpha' = \alpha_1 + \frac{1}{2}\alpha_2, \quad (3)$$

ω_1 is the angel frequency of fundamental wave, d_{eff} is the effective nonlinear coefficient of KTP crystal, c is the speed of light in vacuum, n_1 is the refractive index for fundamental wave, n_2 is the refractive index for second harmonic wave, l is the length of KTP crystal, k_1 is the propagation constant for fundamental wave, α_1 is the absorption coefficient of KTP crystal for fundamental wave, α_2 is the absorption coefficient of KTP crystal for second harmonic wave, $h(\sigma, \beta, \kappa, \xi, \mu)$ is the Boyd-Kleinman focusing factor.

For a standing wave cavity, the second harmonic wave is generated in both directions, thus the cavity reflectance parameter should be modified as

$$r_m = t_{SH}^2 r_2. \quad (4)$$

When the cavity operates on resonance, the reflected power is

$$P_r = \frac{(\sqrt{r_1} - \sqrt{r_m})^2}{(1 - \sqrt{r_1 r_m})^2} P_1. \quad (5)$$

Since r_m depends on P_c through t_{SH} , the impedance matching condition depends on the incident power and the doubling efficiency. The enhancement of the fundamental power on resonance is given by

$$P_c = \frac{t_1}{(1 - \sqrt{r_1 r_m})^2} P_1. \quad (6)$$

This equation is a cubic one in P_c . For a fixed system and the input power level of interest, the doubling efficiencies can be numerically calculated for different losses and transmissions of mirror M_1 .

The second harmonic output power P_2 is

$$P_2 = 2\gamma_{SH} P_c^2 t_{2SH}, \quad (7)$$

t_{2SH} is the power transmission coefficient of the cavity mirrors M_2 for the second harmonic wave.

Based on the parameters of our experimental system, which are listed in Table 1, the functions of the conversion efficiency versus input fundamental power for given losses and input transmission t_1 are numerically calculated. The results are shown in Figs. 2 and 3, respectively.

The experimental setup is shown in Fig. 4. The fundamental light source is a homemade laser diode (LD) pumped ring Nd:YAP laser. The base of the laser housing is an invar steel structure on which a five-mirror ring cavity is built. The solid mechanic configuration provides the basic condition for the stable operation of the laser. The 1080-nm output power up to 1.8 W is obtained with intensity fluctuation of $\pm 0.5\%$. The laser frequency is locked to a temperature well-controlled Fabry-Perot

Table 1. Parameter Values of the Experimental System

Parameter	Value	Parameter	Value
t_1	0.057	n_2	1.777
t_2	0.005	l (m)	0.01
t	0.998	k_1 (m ⁻¹)	1.01×10^7
t_{2SH}	0.9	α_1 (m ⁻¹)	1
ω_1 (s ⁻¹)	1.75×10^{15}	α_2 (m ⁻¹)	1
d_{eff} (esu.)	3.61×10^{-8}	h	0.227
n_1	1.739	γ_{SH} (W ⁻¹)	0.000776

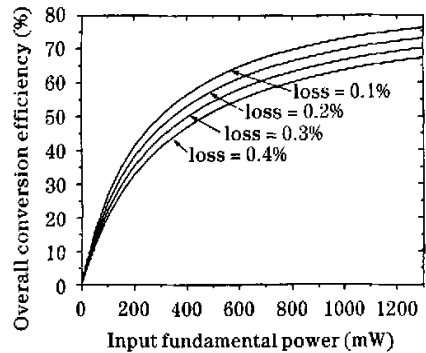


Fig. 2. Total conversion efficiency versus fundamental input power under different losses.

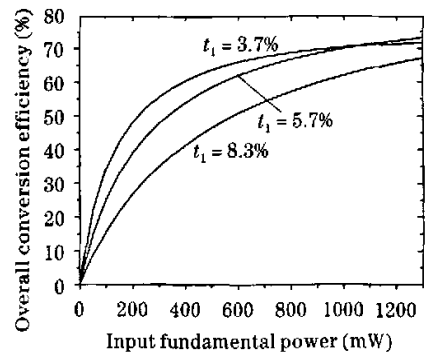


Fig. 3. Total conversion efficiency versus fundamental input power (loss = 0.2%) under different input transmission coefficients.

cavity^[20] (F-P1) with a lock-in amplifier, a proportional integrating (PI) circuit, and a high voltage amplifier. The frequency stabilities of the fundamental laser are better than ± 135 kHz and ± 1.3 MHz in 1 and 30 minutes, respectively, which are monitored by F-P2. The input fundamental power on the doubling cavity can be adjusted by means of a half wave plate (HWP1) and a polarization beam splitter (PBS1). The isolator (ISO) with 38-dB isolation for 1080-nm wave (Model I-106T-5M, from ISOWAVE) is placed between the doubler and the laser to avoid the influence of reflection on the stability of fundamental laser. The doubling cavity with 62 mm length consists of a $3 \times 3 \times 10$ (mm) α -cut KTP crystal (cut along α -axis, and the other two intersection

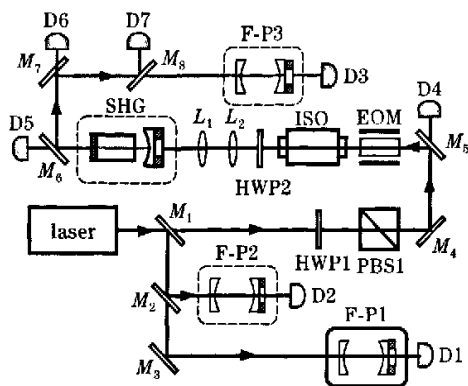


Fig. 4. Experimental setup. SHG: second harmonic generator (doubler); HWP: half wave plate; ISO: optical isolator; EOM: phase modulator; F-P: Fabry-Perot cavity; D: photodiode detector; L: lens; M: mirror.

edges are parallel to b - and c -axis, respectively) and an input mirror. The left facet of KTP is coated for serving as the output mirror of the harmonic wave with the reflection coefficient of 99.5% at 1080 nm and transmission coefficient of 90% at 540 nm. The right facet of KTP is coated antireflection for both 1080 and 540 nm to minimize the intracavity losses. The input mirror of the doubler is a concave mirror with 60-mm radius of curvature and is coated with high reflection for 540 nm and transmission of 5.7% for 1080 nm. The finesse of doubler for the harmonic mode (20) is much smaller than that for the subharmonic modes (75). So for the double resonant cavity, the two overlapping sharp resonant peaks of the subharmonic modes are always involved within the flat resonating envelope of the harmonic mode. In this case, the effect of the frequency dependent phase shift at reflection from dielectric mirrors on the conversion efficiency is not significant. EOM is a phase modulator to modulate the input light for locking the length of doubling cavity to resonate with the input fundamental wave by means of standard sideband technique^[21]. The mode matching between input laser and doubling cavity is adjusted through lenses L_1 and L_2 . A half wave plate (HWP2) is used to adjust the polarization of fundamental wave incident on the KTP crystal to equalize the intensities of two optical modes e_1 and e_2 polarized along b - and c -axis for demonstrating high efficient type-II 90° noncritical phase matching. Because of the birefringence effect, the two optical modes e_1 and e_2 with orthogonal polarizations do not simultaneously resonate in the cavity under general conditions. Around the phase-matching temperature ($\sim 79.5^\circ\text{C}$), slowly adjusting the temperature of KTP and scanning the length of doubling cavity, we can monitor the resonant peaks of e_1 and e_2 modes with an oscilloscope. Once the two peaks overlap, the double resonance of mode e_1 and e_2 in the cavity is reached. In this case, we lock the length of the doubling cavity with standard sideband technique^[21] and stabilize the temperature of KTP on the overlapping point by means of a homemade temperature controller with a precision of 0.003°C . The leakage infrared light from the doubler, which has been phase-modulated with 20-MHz signal frequency, totally passes through the mir-

ror M_6 and then is detected by a photodiode D5. Then the detected photocurrent is mixed with a local signal and generates an error signal. After passing through a PI circuit, this error signal is amplified by a high voltage amplifier. The amplified photocurrent is fed back to the piezoelectric transducer (PZT) mounted on the input mirror of the doubler for locking the cavity on double resonance. The output green light is totally reflected from M_6 . When pump power is increased, the temperature of crystal will be raised and the double resonance might be destroyed. In this case we need to reduce the temperature of the KTP crystal slightly to recover the state of double resonance. To our experience, when the controlling temperature of crystal is decreased about 0.8°C , the double resonance is retrieved.

Figures 5 and 6 are the functions of the harmonic output power and conversion efficiency versus the input fundamental power. The experimental results are in reasonable agreement with the calculated curves. The maximum green output power of 849 mW is obtained when the input fundamental power is 1.18 W. The directly measured doubling efficiency is 72%, if the transmission coefficient of 90% of output mirror is taken into account it should be 80%.

Figures 7 and 8 show the frequency stability of the output green light in 1 and 30 minutes, respectively. The free spectral range of the reference cavity F-P3 for the green

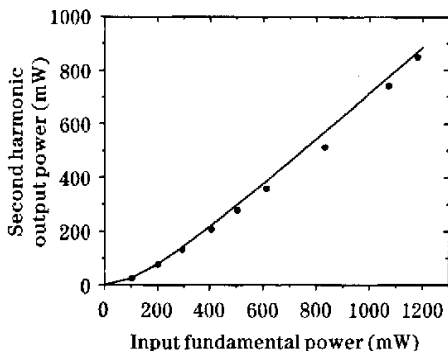


Fig. 5. The output green power versus input fundamental power. Dots: experimental values; solid curve: theoretical calculation.

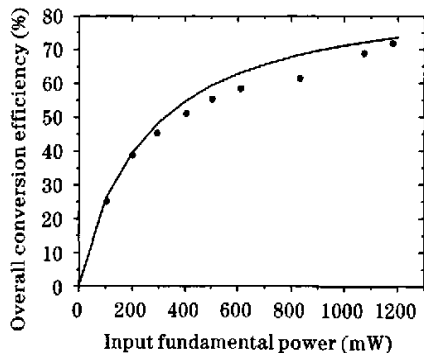


Fig. 6. The frequency-doubling efficiency versus input fundamental power. Dots: experimental values; solid curve: theoretical calculation.

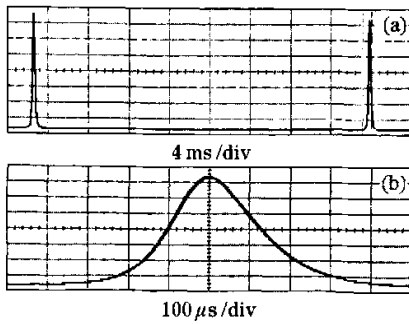


Fig. 7. The green light frequency fluctuation in 1 minute. (a) Whole free spectral range; (b) zoom in one peak.

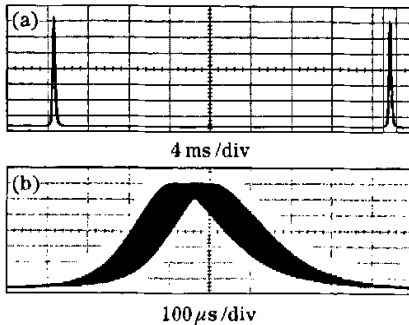


Fig. 8. The green light frequency fluctuation in 30 minutes. (a) Whole free spectral range; (b) zoom in one peak.

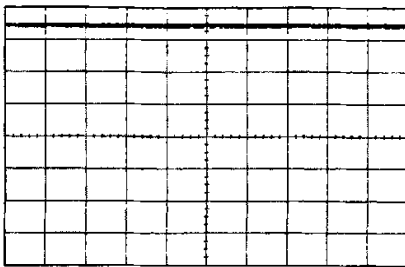


Fig. 9. The green intensity fluctuation in 3 minutes.

light is 1500 MHz. The scanning time recorded by the oscilloscope, which is connected with F-P3, in one free spectral range is 33.2 ms, so the scale of 1 ms on the oscilloscope corresponds to the frequency drift of 45.2 MHz. When both the fundamental laser system and frequency-doubling cavity are locked, the green light frequency stability better than ± 246 kHz in 1 minute and ± 2.3 MHz in 30 minutes are calculated from Figs. 7 and 8, respectively. In Fig. 9, the intensity stability of $\pm 0.65\%$ is shown. The homemade reference cavity F-P3 with invar structure sealed in a polymethyl methacrylate box has good mechanic and thermal stabilities to provide a satisfying frequency standard. According to general methods for measuring frequency stability^[20,22], we measured the relative stability to the reference cavity resonant frequency. In the measured results the effect of the frequency shift of reference cavity has been involved, thus the real stability of the output second harmonic laser is better than the measured value.

A robust frequency-doubler from 1080 to 540 nm is presented. Up to 849-mW harmonic power with good intensity and frequency stabilities is obtained. Since the green light of 540 nm can realize type-II 90° noncritical phase matching in an α -cut KTP crystal, the walk-off effect and the polarization mixing effect between two polarizing nondegenerate fundamental modes can be minimized. The presented high stable frequency-doubler has potential applications in the experimental quantum optics and quantum information.

This research was supported by the Major State Basic Research Project of China (No. 2001CB3099304), the National Natural Science Foundation of China (No. 60238010, 60178012, 60378014), and Shanxi Provincial Science Foundation (No. 20041038). Q. Pan is the author to whom the correspondence should be addressed, his e-mail address is panqing@sxu.edu.cn.

References

1. Q. Pan, Y. Zhang, T. Zhang, C. Xie, and K. Peng, *J. Phys. D: Appl. Phys.* **30**, 1588 (1997).
2. H. Wang, Y. Zhang, Q. Pan, H. Su, A. Porzio, C. Xie, and K. Peng, *Phys. Rev. Lett.* **82**, 1414 (1999).
3. K. C. Peng, Q. Pan, H. Wang, Y. Zhang, H. Su, and C. D. Xie, *Appl. Phys. B* **66**, 755 (1998).
4. Z. Y. Ou, S. F. Pereira, H. J. Kimble, and K. C. Peng, *Phys. Rev. Lett.* **68**, 3663 (1992).
5. X. Li, Q. Pan, J. Jing, J. Zhang, C. Xie, and K. Peng, *Phys. Rev. Lett.* **88**, 047904 (2002).
6. X. Jia, X. Su, Q. Pan, J. Gao, C. Xie, and K. Peng, *Phys. Rev. Lett.* **93**, 250503 (2004).
7. J. Gao, H. Wang, M. Huang, C. Xie, K. Peng, Z. Yu, C. Ma, and X. Wang, *Appl. Opt.* **34**, 1519 (1995).
8. K. I. Martin, W. A. Clarkson, and D. C. Hanna, *Opt. Lett.* **21**, 875 (1996).
9. K. I. Martin, W. A. Clarkson, and D. C. Hanna, *Appl. Opt.* **36**, 4149 (1997).
10. Q. Pan, T. Zhang, Y. Zhang, R. Li, K. Peng, Z. Yu, and Q. Lu, *Appl. Opt.* **37**, 2394 (1998).
11. X. Li, Q. Pan, J. Jing, C. Xie, and K. Peng, *Opt. Commun.* **201**, 165 (2002).
12. Z. Y. Ou, S. F. Pereira, E. S. Polzik, and H. J. Kimble, *Opt. Lett.* **17**, 640 (1991).
13. K. Hayasaka, Y. Zhang, and K. Kasai, *Opt. Express* **12**, 3567 (2004).
14. Z. Y. Ou and H. J. Kimble, *Opt. Lett.* **18**, 1053 (1993).
15. G. Breitenbach, S. Schiller, and J. Mlynek, *J. Opt. Soc. Am. B* **12**, 2095 (1995).
16. R. Paschotta, P. Kürz, R. Henking, S. Schiller, and J. Mlynek, *Opt. Lett.* **19**, 1325 (1994).
17. A. Ashkin, G. D. Boyd, and J. M. Dziedzic, *IEEE J. Quantum Electron.* **2**, 109 (1966).
18. W. J. Kozlovsky, C. D. Nabors, and R. L. Byer, *IEEE J. Quantum Electron.* **24**, 913 (1988).
19. G. D. Boyd and D. A. Kleinman, *J. Appl. Phys.* **39**, 3597 (1968).
20. F. Zhao, Q. Pan, and K. Peng, *Chin. Opt. Lett.* **2**, 334 (2004).
21. R. W. P. Drever, J. L. Hall, F. V. Kowalski, J. Hough, G. M. Ford, A. J. Munley, and H. Ward, *Appl. Phys. B* **31**, 97 (1983).
22. K.-C. Peng, L.-A. Wu, and H. J. Kimble, *Appl. Opt.* **24**, 938 (1985).

with high output power

作者: Yu Luo, Ying Li, Changde Xie, Kunchi Peng, Qing Pan
作者单位: State Key Laboratory of Quantum Optics and Quantum Optics Devices, Institute of Opto-Electronics of Shanxi University, Taiyuan 030006
刊名: 中国光学快报 (英文版) ISTIC EI SCI
英文刊名: CHINESE OPTICS LETTERS
年, 卷(期): 2005, 3(7)

参考文献(22条)

1. Q Pan;Y Zhang;T Zhang;C Xie, and K Peng [查看详情](#) 1997
2. H Wang;Y Zhang;Q Pan;H Su, A Porzio, C Xie, and K Peng [查看详情](#) 1999
3. K C Peng;Q Pan;H Wang;Y Zhang, H Su, and C D Xie [查看详情](#) 1998
4. Z Y Ou;S F Pereira;H J Kimble;K C Peng [查看详情](#) 1992
5. X Li;Q Pan;J Jing;J Zhang, C Xie, and K Peng [查看详情](#) 2002
6. X Jia;X Su;Q Pan;J Gao, C Xie, and K Peng [查看详情](#) 2004
7. J Gao;H Wang;M Huang;C Xie, K Peng, Z Yu, C Ma, and X Wang [查看详情](#) 1995
8. K I Martin;W A Clarkson;D C Hanna [查看详情](#) 1996
9. K I Martin;W A Clarkson;D C Hanna [查看详情](#) 1997
10. Q Pan;T Zhang;Y Zhang;R Li, K Peng, Z Yu, and Q Lu [查看详情](#) 1998
11. X Li;Q Pan;J Jing;C Xie, and K Peng [查看详情](#) 2002
12. Z Y Ou;S F Pereira;E S Polzik;H J Kimble [查看详情](#) 1991
13. K Hayasaka;Y Zhang;K Kasai [查看详情](#) 2004
14. Z Y Ou;H J Kimble [查看详情](#) 1993
15. G Breitnbach;S Schiller;J Mlynek [查看详情](#) 1995
16. R Paschotta;P Kürz;R Henking;S Schiller, and J Mlynek [查看详情](#) 1994
17. A Ashkin;G D Boyd;J M Dziedzic [查看详情](#) 1966
18. W J Kozlovsky;C D Nabors;R L Byer [查看详情](#) 1988
19. G D Boyd;D A Kleinman [查看详情](#) 1968
20. F Zhao;Q Pan;K Peng [Improving frequency stability of laser by means of temperature-controlled Fabry-Perot cavity](#)[期刊论文]-[Chinese Optics of Letters](#) 2004(02)
21. R W P Drever;J L Hall;F V Kowalski;J Hough, G M Ford, A J Munley, and H Ward [查看详情](#) 1983
22. K -C Peng;L -A Wu;H J Kimble [查看详情](#) 1985

引用本文格式: Yu Luo, Ying Li, Changde Xie, Kunchi Peng, Qing Pan [Frequency-stabilized semimonolithic frequency doubler with high output power](#)[期刊论文]-[中国光学快报 \(英文版\)](#) 2005(7)